JACS
JOURNAL OF THE AMERICAN CHEMICAL SOCIETY

Communication

pubs.acs.org/JACS

Oxidation Mechanism of Formic Acid on the Bismuth Adatom-Modified Pt(111) Surface

Juan Victor Perales-Rondón,[†] Adolfo Ferre-Vilaplana,[‡,§] Juan M. Feliu,[†] and Enrique Herrero*[,†]

[†]Instituto de Electroquímica, Universidad de Alicante, Apdo. 99, E-03080 Alicante, Spain

[‡]Instituto Tecnológico de Informática, Ciudad Politécnica de la Innovación, Camino de Vera s/n, E-46022 Valencia, Spain

[§]Departamento de Sistemas Informáticos y Computación, Escuela Politécnica Superior de Alcoy, Universidad Politécnica de Valencia, Plaza Ferrándiz y Carbonell s/n, E-03801 Alcoy, Spain

Supporting Information

ABSTRACT: In order to improve catalytic processes, elucidation of reaction mechanisms is essential. Here, supported by a combination of experimental and computational results, the oxidation mechanism of formic acid on Pt(111) electrodes modified by the incorporation of bismuth adatoms is revealed. In the proposed model, formic acid is first physisorbed on bismuth and then deprotonated and chemisorbed in formate form, also on bismuth, from which configuration the C−H bond is cleaved, on a neighbor Pt site, yielding CO_2. It was found computationally that the activation energy for the C−H bond cleavage step is negligible, which was also verified experimentally.

Cleaner energy based on the oxidation of small organic molecules (i.e., formic acid, methanol, ethanol, etc.) in fuel cells requires efficient electrocatalysts capable of operating at low overpotentials and high current densities. To guide the development of optimal catalysts, the oxidation mechanisms of the fuels have to be fully understood. The oxidation of formic acid to CO_2, involving the exchange of only two electrons and the cleavage of a single C−H bond, is probably the simplest among the processes considered.[1,2] In order to activate the aforementioned C−H bond cleavage, platinum surfaces are particularly effective, giving rise to overpotentials lower than those observed in the oxidation of small organic molecules on others metals. However, even on pure platinum, the measured oxidation currents, at low overpotentials, are still low. To increase the activity of the catalyst, modifications of platinum with other elements have been proposed. Intermetallic PtBi nanoparticles have shown an excellent performance, where high currents at very low overpotentials have been recorded.[3−6] Nevertheless, the role played by Bi, or any other modifier, in the considered oxidation process is still unknown. In this work, using a combination of DFT calculations and experimental results on single-crystal electrodes, the electro-oxidation mechanism of formic acid on the bismuth adatom-modified Pt(111) surface is completely elucidated. Note that single-crystal electrodes allow direct comparison between computational and experimental results.

The electrooxidation of formic acid on pure platinum electrodes can evolve following two main routes: through CO, which remains strongly adsorbed on the electrode, and thus is difficult to oxidize, and through an active intermediate, which is the desired route.[2,7] For this route, the nature of the intermediate is still under discussion.[8−13] Electrocatalytic reaction rates depend on the surface structure of the electrodes. So, Pt(111) electrodes exhibit low activity through the active intermediate and negligible CO formation, whereas Pt(100) surfaces show the highest activity for both routes.[14,15] Moreover, to increase the reaction rate through the direct route, pure platinum electrodes have been modified incorporating other species. Bismuth has given rise to very promising results.[16−18] The addition of Bi adatoms to pristine Pt(111) single-crystal electrodes diminishes the overpotentials and increases the current density up to 30−40 times that measured for the unmodified surface.[15] Such improvement is clearly related to the deposition of Bi on the terraces, since it reaches the maximum for coverages close to the saturation value. For low and moderate Bi coverages, only isolated or <1 nm islands have been seen by scanning tunneling microscopy, which supports the random distribution model of adatoms on the surface.[19] Also, statistical models suggest that a Bi−Pt ensemble would be the reactive site, although the role played by each atom in the considered oxidation process has not yet been described.[20]

It has been pointed out that adsorbed formate plays an important role in the process of oxidation of formic acid on pure platinum electrodes. This species has been detected by FTIR[9−13] and voltammetry,[21] showing that the onset for the oxidation process coincides with that for the adsorption of formate.[21] Also, density functional theory calculations indicate that adsorbed formate is a key part of the considered oxidation process.[22,23] More specifically, it has been suggested that adsorbed formate facilitates the adsorption of a new formic acid (or formate) molecule with the C−H bond directed toward the surface.[24] From such a configuration, the activation energy for the cleavage of the C−H bond would be low (ca. 0.5 eV), yielding CO_2 as the final product. To adsorb the formate−formic dimer, a Pt ensemble with several Pt atoms is required. Thus, the initial hypothesis could be that bismuth facilitates the adsorption of formate on Pt sites.

To detect adsorption of formate on single-crystal electrodes, fast-scan voltammetry can be used.[21] During formic acid

Received: June 13, 2014
Published: September 4, 2014

dx.doi.org/10.1021/ja505943h | J. Am. Chem. Soc. 2014, 136, 13110−13113

oxidation, voltammetric currents come from two different processes: the oxidation process itself and adsorption processes (mainly hydrogen and anions) on the electrode surface. At low scan rates, oxidation currents are much higher than adsorption currents. However, adsorption currents are proportional to the scan rate, whereas oxidation currents are much less affected by the scan rate.[18] By using high scan rates, adsorption currents can dominate the voltammetric profile.[21] For a Bi adatom-modified Pt(111) electrode with a coverage of 0.25, which is very close to the maximum activity, both types of experiments (low and high scan rate voltammetry) are shown in Figure 1.

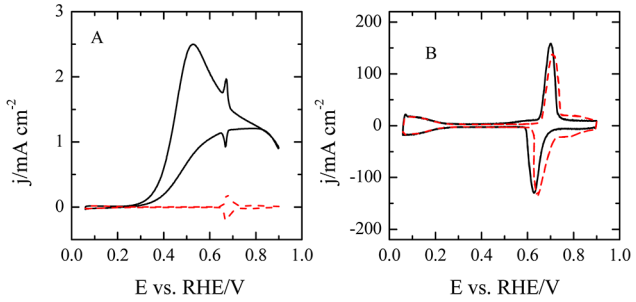

Figure 1. Voltammetric profiles of Bi−Pt(111) electrode with θ_{Bi} = 0.25 in 0.5 M $HClO_4$ + 0.05 M HCOOH (full line) and 0.5 M $HClO_4$ (dashed lines) at (A) 0.05 and (B) 50 V/s.

The same kinds of experimental results are shown in the Supporting Information, Figures S1−S3, for the bare electrode and two additional coverages. As can be seen by comparison of the voltammetries in presence and absence of formic acid, at 50 mV/s (Figures 1A and S1A−S3A), adsorption currents are much smaller than those corresponding to formic acid oxidation, the shape of the voltammogram indicating an irreversible oxidation process that is inhibited at high potentials. At high bismuth coverages and above 0.5 V, the incoming molecules are immediately oxidized on the electrode.

However, at 50 V/s (Figures 1B and S1B−S3B), adsorption currents have increased 3 orders of magnitude, making adsorption the dominant process recorded in the voltammetry. In presence of formic acid, the voltammograms are practically symmetrical through the potential axis, which indicates that currents are mainly due to adsorption processes, and thus, the contribution from oxidation processes can be discarded. Comparison with the voltammograms measured in the absence of formic acid enables us to establish the formate adsorption range on platinum. In perchloric acid solutions, a hydrogen adsorption region appears at potentials below 0.3 V, whereas bismuth redox give rise to a pair of peaks between 0.6 and 0.7 V, in a similar way to what is found at 50 mV/s (Figures 1B and S4). Above 0.7 V, the signals corresponding to OH adsorption on Pt sites can be detected. In presence of formic acid at 50 V/s, some changes can be observed in the voltammograms. First, depending on the coverage, a signal corresponding to formate adsorption can be seen between 0.4 and 0.6 V in the positive scan direction (Figure S5). In Figure 1B, since bismuth coverage is high, the amount of free Pt sites is small, and therefore, the total amount of adsorbed formate on platinum is also small. However, in Figure S5, the signal corresponding to formate adsorption diminishes as the coverage increases. For bismuth-modified surfaces, the voltammograms in the presence of formic acid at 50 V/s are almost identical to those measured in sulfuric acid solutions in the absence of formic acid, which corroborates that these processes are due to the adsorption of the formate anion.[25] As the amount of bismuth coverage increases, the onset for the formate anion adsorption is displaced toward higher potential values (see Figure S5).[26] In parallel to the appearance of the new signal between 0.4 and 0.6 V, those signals corresponding to the adsorption of OH above 0.7 V disappear, and a small shift in the bismuth redox peaks is observed. All these results indicate that, for θ_{Bi} = 0.25, formate is present on platinum sites only above 0.5 V, whereas on the unmodified Pt(111) electrode it can be detected at 0.35 V.[21] On the other hand, the onset potential for formic acid oxidation diminishes as the bismuth coverage increases. Thus, it is clear that the catalytic effect of bismuth is not linked to the adsorption of formate on Pt sites.

In order to gain insight into the mechanisms explaining the higher performance of bismuth modified electrodes, DFT calculations, modeling different aspects of the investigated process, were carried out. Adsorption of bismuth on fcc and hcp sites of the Pt(111) surface was found to be favorable by 3.20 and 3.17 eV, respectively. The adsorption of bismuth causes a redistribution of electron density on the bare surface. The results corresponding to fcc sites are displayed in Figure 2;

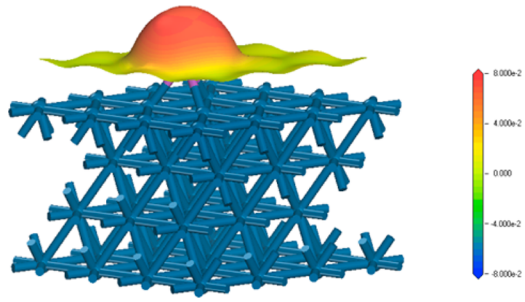

Figure 2. Electrostatic potential [Ha/e] mapped on electron isodensity surface for a density value ρ = 0.01 e/Å^3 for a Bi adatom adsorbed on the Pt(111) surface.

the ones corresponding to hcp sites are virtually identical. From Figure 2, it can be inferred that an excess of positive charge would be concentrated on the adatom, while the compensating negative charge would be distributed among the platinum atoms close to the adatom. Thus, bismuth has cationic character when adsorbed on Pt(111). Here we propose that the formation of the identified cationic site determines the oxidation process of formic acid on the Bi−Pt(111) surface, driving its mechanism.

It was found that physisorption of hydrated formic acid near the adatom is favorable by ca. 0.26 eV. In its lower energy configuration, the carbonyl group is directed toward the adatom (Figure S6), with changes in the bonds geometry being observed. In such a configuration, the O−H distance of the carboxylic group increases, whereas the distance to the corresponding hydrogen bond diminishes as compared to the distances calculated in absence of surface. Adatoms favoring physisorption of formic acid in the C−H down configuration have been previously found,[27] though the evolution of formic acid on the adatom site was not studied, and only the generic argument that the configuration facilitates the cleavage of the C−H bond is provided. Here, the relevance of the role played by the adatom during the oxidation process is established, and the complete oxidation mechanism is revealed.

dx.doi.org/10.1021/ja505943h | J. Am. Chem. Soc. 2014, 136, 13110−13113

From the described physisorbed configuration, the deprotonation of the formic acid molecule would be assisted by the fact that, from this location, formate was found to be favorably chemisorbed by 0.39 eV on the bismuth adatom without barrier. Therefore, the two processes of formic acid deprotonation and formate chemisorption on bismuth would take place simultaneously. The above-described physisorption- and formate chemisorption-related observations suggest that the pK_a of formic acid near the surface would be lower than that in the bulk. Physisorption, deprotonation, and formate chemisorption would all be driven by the positive charge located on the adatom.

Once formate chemisorption on the adatom has taken place, it was assumed that the electron in excess exits toward the circuit. So, the evolution of the HCOO fragment bonded to the bismuth modified platinum surface was analyzed. Running quantum mechanical molecular dynamics simulations, it was found that, transiting among different configurations whose energies fluctuate within the error of the calculations, the chemisorbed HCOO fragment evolves in a rotating process for which the Bi−O and O−C bonds play the role of rotation axis, until a sufficiently favorable C−H down configuration is reached. From this configuration the C−H bond is cleaved to yield CO_2 and an adsorbed H atom (Figure 3). The activation

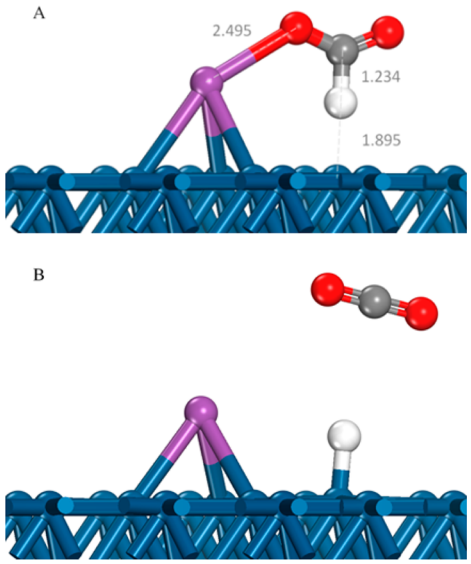

Figure 3. (A) HCOO fragment adsorbed on the Bi−Pt(111) surface and (B) final products in the oxidation of formic acid.

energy estimated from the calculations for the C−H bond cleavage step was negligible, presenting a favorable energy of 1.21 eV. Comparison with previous results on unmodified Pt(111) electrodes[24] shows a significant diminution in activation energy for the C−H bond cleavage step, from 0.5 to 0 eV.

In summary, the oxidation reaction model proposed here draws a bifunctional catalyst in which the bismuth adatom plays a determinant role in the formic acid adsorption and evolution to chemisorbed formate, whereas an adjacent Pt site is responsible for the cleavage of the C−H bond, which is in agreement with previous analysis suggesting that the catalytic site is a Bi−Pt ensemble.[20]

To corroborate the proposed reaction mechanism, activation energies for different bismuth coverages on Pt(111) electrodes were experimentally estimated. To do so, voltammetric profiles for the oxidation process were recorded at different temperatures (Figure 4A). Since CO formation on these electrodes is

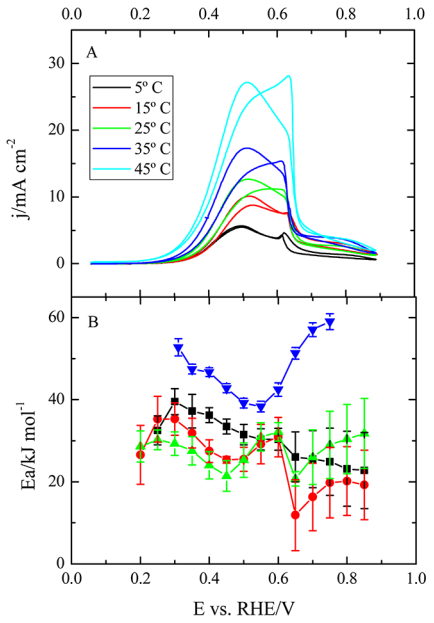

Figure 4. (A) Voltammetric profile of a Bi−Pt(111) electrode with θ_{Bi} = 0.25 in 0.5 M H_2SO_4 + 0.1 M HCOOH at 0.05 V/s at different temperatures. (B) Measured activation energy for different Bi coverages θ_{Bi}: (▼) 0.00, (■) 0.10, (●) 0.22, and (▲) 0.28.

negligible,[15,17] the measured currents correspond to the direct route. So, the logarithm of the current density at constant potential can be charted vs T^{-1} in an Arrhenius plot to determine the apparent activation energy (Figure S7). Activation energies vs electrode potentials for different bismuth coverages are displayed in Figure 4B. For comparison, the activation energy for the unmodified Pt(111) electrode is also included. For the bare electrode, the activation energy was determined from the intrinsic activity of the electrode through the active intermediate reaction measured at different temperatures.[14,15]

In Figure 4B, as bismuth coverage increases, a significant diminution in the activation energy of the process can be observed. For the electrode with the highest activity, the diminution is around 20 kJ/mol with respect to that corresponding to the unmodified Pt(111) electrode. It should be borne in mind that experimentally estimated activation energies are apparent activation energies, which are a combination of the activation energies of all the different steps involved in a mechanism, whereas computationally estimated activation energies correspond to a single step in a process. Additionally, in the case of the bismuth-modified Pt(111) electrodes, the measured activation energy is an average of the activation energies for all the different kinds of reactive sites on the surface. For the investigated surfaces, two different kinds of active sites are considered: the Pt−Bi ensemble of Figure 3, and the Pt ensemble on which the reaction occurs through the formate−formic dimer. If the activation energy for the Pt−Bi ensemble is much lower than that for the Pt sites, it is clear that the measured activation energy should diminish when increasing bismuth coverage, as found experimentally. For the bismuth coverage with the

dx.doi.org/10.1021/ja505943h | J. Am. Chem. Soc. 2014, 136, 13110−13113

highest catalytic activity (θ_{Bi} = 0.28), the measured activation energy is not zero because of the contribution of other previous steps and also from some Pt ensembles still accessible on the surface. At 0.45 V, the measured activation energy for θ_{Bi} = 0.28 is 21 kJ/mol, whereas on the unmodified surface it is 42 kJ/mol. From these data, the contribution of the different steps/processes to the apparent activation energy at this bismuth coverage can be estimated. Since each bismuth adatom blocks three platinum sites, at the considered coverage, the number of free Pt sites is 0.16. This implies that the contribution of these sites to the total energy would be 0.16 × 42 = 6.7 kJ/mol. The remaining 14.3 kJ/mol (or 0.15 eV) should arise, then, from the previous steps for the reaction on the Bi−Pt ensemble, probably from the deprotonation of the formic acid close to the Bi adatom to give rise to formate, which will adsorb immediately on the Bi adatom.

Finally, it should be stressed that the reaction mechanism suggested by our DFT calculations is in very good agreement with a broad set of experimental data. First, unlike the Pt(111) electrodes, for which currents increase with the pH,[12] the currents measured on the bismuth-modified Pt(111) electrodes do not depend on the pH for values between 0 and 2,[18] which implies that the formic acid molecule is the reactant species at these pH values. As has been shown, a formic acid molecule close to the Bi adatom would have a lower pK_a, which would facilitate its adsorption as formate on the bismuth adatom; therefore, the presence of a formate molecule close to the adatom is not required. Second, the activation energy diminishes with the bismuth coverage. Third, the proposed reaction mechanism helps to explain why the onset of the reaction is between 0.2 and 0.3 V for the different bismuth coverages. In the final step, adsorbed hydrogen is formed, "poisoning" the active site. In order to reactivate the active site, hydrogen should be desorbed. Thus, a steady current for formic acid oxidation is possible only at potentials at which hydrogen is easily desorbed from the Pt sites, that is, where hydrogen equilibrium coverage on the surface is low. On the unmodified Pt(111) surface, hydrogen coverage is low above 0.30 V, and this potential value diminishes as the bismuth coverage increases (see Figure S4). Thus, the onset potential for the reaction shifts accordingly. And, fourth, the proposed mechanism also explain why the activation energy diminishes from 0.2 to 0.5 V. Hydrogen desorption also contributes to the measured activation energy, since it can be considered also the first step in the reaction at potentials where hydrogen is adsorbed. As the potential is made more positive, this step is faster (i.e., with a lower activation energy), which results in a diminution of the overall activation energy. As a conclusion, it can be verified that the computational results presented here are in very good agreement with a broad set of experimental data, thus explaining them, which rigorously supports the proposed reaction model.

■ ASSOCIATED CONTENT

Supporting Information

Experimental details, computational methods, and additional figures. This material is available free of charge via the Internet at http://pubs.acs.org.

■ AUTHOR INFORMATION

Corresponding Author

herrero@ua.es

Notes

The authors declare no competing financial interest.

■ ACKNOWLEDGMENTS

This work has been financially supported by the MINECO (Spain) (project CTQ2013-44083-P) and Generalitat Valenciana (project PROMETEOII/2014/013).

■ REFERENCES

(1) Parsons, R.; Vandernoot, T. *J. Electroanal. Chem.* **1988**, *257*, 9.
(2) Koper, M. T. M.; Lai, S. C. S.; Herrero, E. In *Fuel cell catalysis, a surface science approach*; Koper, M. T. M., Ed.; John Wiley & Sons, Inc.: Hoboken, NJ, 2009; p 159.
(3) Roychowdhury, C.; Matsumoto, F.; Zeldovich, V. B.; Warren, S. C.; Mutolo, P. F.; Ballesteros, M.; Wiesner, U.; Abruña, H. D.; Disalvo, F. J. *Chem. Mater.* **2006**, *18*, 3365.
(4) Roychowdhury, C.; Matsumoto, F.; Mutolo, P. F.; Abruna, H. D.; DiSalvo, F. J. *Chem. Mater.* **2005**, *17*, 5871.
(5) Casado-Rivera, E.; Gal, Z.; Angelo, A. C. D.; Lind, C.; DiSalvo, F. J.; Abruna, H. D. *ChemPhysChem* **2003**, *4*, 193.
(6) Blasini, D. R.; Rochefort, D.; Fachini, E.; Alden, L. R.; DiSalvo, F. J.; Cabrera, C. R.; Abruna, H. D. *Surf. Sci.* **2006**, *600*, 2670.
(7) Feliu, J. M.; Herrero, E. In *Handbook of fuel cells—fundamentals, technology and applications*; Vielstich, W., Gasteiger, H., Lamm, A., Eds.; John Wiley & Sons, Ltd.: Chichester, 2003; Vol. 2.
(8) Samjeske, G.; Miki, A.; Ye, S.; Osawa, M. *J. Phys. Chem. B* **2006**, *110*, 16559.
(9) Chen, Y. X.; Ye, S.; Heinen, M.; Jusys, Z.; Osawa, M.; Behm, R. J. *J. Phys. Chem. B* **2006**, *110*, 9534.
(10) Cuesta, A.; Cabello, G.; Gutierrez, C.; Osawa, M. *Phys. Chem. Chem. Phys.* **2011**, *13*, 20091.
(11) Osawa, M.; Komatsu, K.; Samjeske, G.; Uchida, T.; Ikeshoji, T.; Cuesta, A.; Gutierrez, C. *Angew. Chem., Int. Ed.* **2011**, *50*, 1159.
(12) Joo, J.; Uchida, T.; Cuesta, A.; Koper, M. T. M.; Osawa, M. *J. Am. Chem. Soc.* **2013**, *135*, 9991.
(13) Chen, Y. X.; Heinen, M.; Jusys, Z.; Behm, R. J. *Langmuir* **2006**, *22*, 10399.
(14) Grozovski, V.; Climent, V.; Herrero, E.; Feliu, J. M. *ChemPhysChem* **2009**, *10*, 1922.
(15) Grozovski, V.; Climent, V.; Herrero, E.; Feliu, J. M. *Phys. Chem. Chem. Phys.* **2010**, *12*, 8822.
(16) Clavilier, J.; Fernández-Vega, A.; Feliu, J. M.; Aldaz, A. *J. Electroanal. Chem.* **1989**, *258*, 89.
(17) Herrero, E.; Fernández-Vega, A.; Feliu, J. M.; Aldaz, A. *J. Electroanal. Chem.* **1993**, *350*, 73.
(18) Maciá, M. D.; Herrero, E.; Feliu, J. M. *J. Electroanal. Chem.* **2003**, *554*, 25.
(19) Kim, J.; Rhee, C. K. *Electrochem. Commun.* **2010**, *12*, 1731.
(20) Leiva, E.; Iwasita, T.; Herrero, E.; Feliu, J. M. *Langmuir* **1997**, *13*, 6287.
(21) Grozovski, V.; Vidal-Iglesias, F. J.; Herrero, E.; Feliu, J. M. *ChemPhysChem* **2011**, *12*, 1641.
(22) Neurock, M.; Janik, M.; Wieckowski, A. *Faraday Discuss.* **2009**, *140*, 363.
(23) Gao, W.; Keith, J. A.; Anton, J.; Jacob, T. *J. Am. Chem. Soc.* **2010**, *132*, 18377.
(24) Wang, H.-F.; Liu, Z.-P. *J. Phys. Chem. C* **2009**, *113*, 17502.
(25) Clavilier, J.; Feliu, J. M.; Aldaz, A. *J. Electroanal. Chem.* **1988**, *243*, 419.
(26) Climent, V.; Herrero, E.; Feliu, J. M. *Electrochem. Commun.* **2001**, *3*, 590.
(27) Peng, B.; Wang, H.-F.; Liu, Z.-P.; Cai, W.-B. *J. Phys. Chem. C* **2010**, *114*, 3102.